THE JOURNAL OF PHYSICAL CHEMISTRY C LETTERS

2008, *112,* 8136–8139
Published on Web 05/01/2008

Structural Evaluation along the Nanotube Length for Super-long Vertically Aligned Double-Walled Carbon Nanotube Arrays

Supriya Chakrabarti, Kuanping Gong, and Liming Dai*

Department of Chemical and Materials Engineering, University of Dayton, 300 College Park, Dayton, Ohio 45469

Received: March 8, 2008; Revised Manuscript Received: April 3, 2008

By performing Raman spectroscopic and electrochemical measurements along the nanotube length, we have demonstrated that there is a concentration gradient of structural defects along the tube length for super-long (ca. 5 mm) vertically aligned double-walled carbon nanotubes (SLVA-DWNTs) produced by water-assisted CVD growth. An increase in the structural defect content along the nanotube length from the top to bottom end was observed in the present study due to the "bottom growth" process and the decay of the catalyst reactivity with the growth time. The newly observed defect content gradient facilitated us to tune the nanotube electrochemistry along its length and to deposit metal particles in a length-specific fashion.

Recent advances in chemical vapor deposition (CVD) techniques have facilitated the growth of super-long vertically aligned carbon nanotubes (SLVA-CNTs) with millimiter-order lengths.[1–3] SLVA-CNTs offer significant advantages over their shorter counterparts for various potential applications, including multifunctional composites,[4,5] sensors,[6–8] and nanoelectronics.[9,10] In addition, their millimeter-order lengths provide novel opportunities for translating electronic, thermal, and other physical properties through individual nanotubes over large length scales. As such, the large-scale structural and property uniformity along the nanotube length is important for many novel applications involving super-long carbon nanotubes. Therefore, structural evaluation along the nanotube length for SLVA-CNTs is of both fundamental and applied significance.

Defects inevitably form during the nanotube growth, especially for super-long nanotubes that require a prolonged growth process.[1–3] The introduction of any defects, including topological disorders, substitutional impurities, and side-wall vacancies, during the growth process would ultimately affect the resultant nanotube properties ranging from electronic characteristics to chemical activities.[11–14] Knowledge of the defect distribution along the tube length is essential to understand the structure−property relationship of super-long carbon nanotubes for potential applications. As far as we are aware, no such study has been reported. In this Letter, we report our recent study on the use of Raman spectroscopy, electron microscopy, and electrochemical cyclic voltammetry for probing structural defects along the nanotube length for 5-mm-long vertically aligned double-walled carbon nanotubes (SLVA-DWNTs). Significant variation in defect distribution was observed along the nanotube length.

With only one additional graphene coaxial tube around the core of a single-walled carbon nanotube (SWNT), DWNTs can largely preserve the SWNT characteristics. Unlike the SWNT, however, the outer wall of a DWNT could prevent its inner core from possible detrimental damage caused by chemical modification while allowing functional moieties to be confined onto the nanotube surface. The 5-mm-long SLVA-DWNTs were synthesized onto a Si/SiO_2 wafer from Fe catalyst by the water-assisted CVD technique using high-purity (99.99%) ethylene as the carbon source and helium/H_2 (2.5:1 v/v) as a carrier gas under 1 atm pressure at 700 °C for about 10 h. A thin (10 nm) Al_2O_3 buffer film was used between the Si/SiO_2 substrate and the Fe catalyst layer (1 nm thick). During the nanotube growth process, a controlled amount of water vapor was also introduced into the carrier gas at concentrations in the range of 200 to 400 ppm. The SLVA-DWNT arrays were produced under the optimized conditions, as described elsewhere.[1–3]

Figure 1a shows a typical optical microscopic image for a 5-mm-long SLVA-DWNT array. The corresponding scanning electron microscope (SEM, a Hitachi S-4800 high resolution SEM unit) images under different magnifications given in Figure 1b and c clearly show the well-aligned individual nanotubes closely packed together. Transmission electron microscope (TEM, a Hitachi H-7600 TEM unit) observations of the same nanotube sample confirmed that most of the constituent CNTs possess a double-walled structure with an average outer diameter of 4 nm (Figure 1d and e).

Figure 2 shows the thermogravimetric analysis (TGA, TA Instrument TGA Q 50) data for the as-grown SLVA-DWNT sample in oxygen. As can be seen, no weight loss was observed at temperatures below 550 °C, indicating that the SLVA-DWNTs are thermally stable and free from amorphous carbon impurities that physically deposited onto the nanotube surface. The very narrow decomposition range between about 550 and 700 °C with an almost 100% weight loss indicates that very pure double-walled nanotubes have been produced even without residual metal nanoparticles. Because of the "bottom growth" process, the metal catalyst nanoparticles have, most probably, been left over on the substrate surface upon removal of the nanotube bunches for the TGA measurements.

* Corresponding Author. E-mail: ldai@udayton.edu

10.1021/jp802059t CCC: $40.75

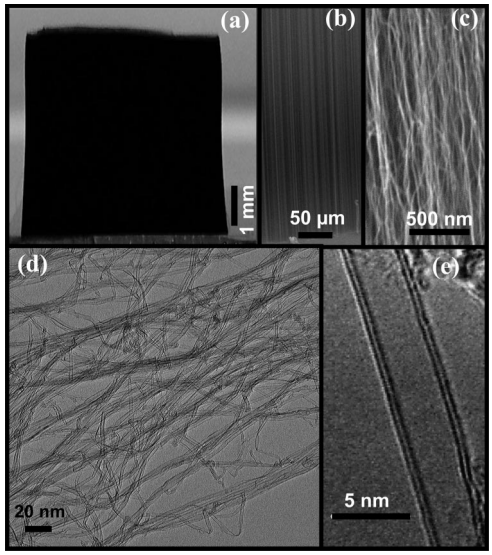

Figure 1. SLVA-DWNTs synthesized by the water-assisted CVD technique: (a) a digital photograph of the 5-mm-long SLVA-DWNT array, (b and c) cross-sectional scanning electron microscope (SEM) images of the SLVA-DWNTs under different magnifications, (d) a transmission electron microscope (TEM) image of the super-long DWNTs, and (e) a high-resolution TEM image of an individual super-long DWNT.

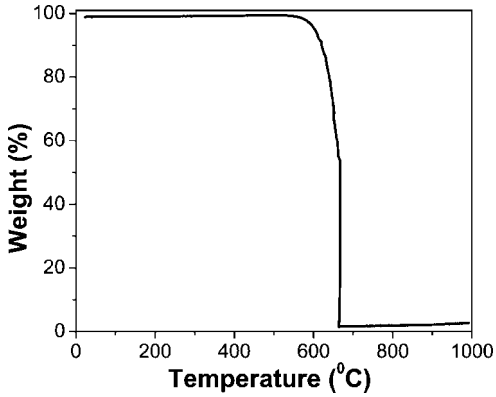

Figure 2. Thermogravimetric data (ramp rate 20 °C/min) of 1.5 mg SLVA-DWNT sample in O_2.

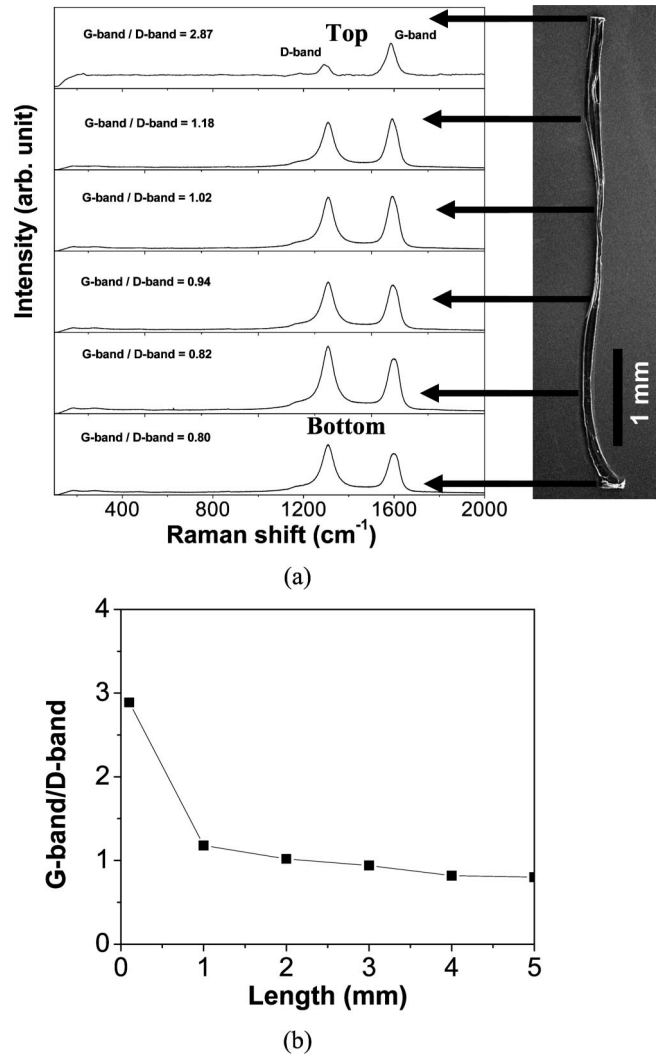

Figure 3. (a) Raman spectra of the 5-mm-long DWNT bunch, showing the variation of G-band to D-band ratio from the bottom to top end along the nanotube length. (b) Plot of the G-band to D-band peak ratio vs the nanotube length from the top to bottom end for the 5-mm-long SLVA-DWNT bunch.

Micro-Raman spectroscopy serves as a convenient tool for investigating the defect distribution along the nanotube length for the super-long DWNTs. To perform Raman spectroscopic measurements (514 nm, RENISHAW inVia) along the tube length with ~1 mm intervals, we have taken small bunches of long nanotubes out from the as-grown SLVA-DWNT arrays and measured at each of the length intervals for at least 6 times with 10-s integration for each of the measurements to minimize statistic errors. As shown in Figure 3a, the G-band to D-band ratio for the 5-mm-long SLVA-DWNTs decreases gradually from the top to bottom tube end, indicating that the defect content at the top end is much lower than that of the bottom end. The G-band represents the graphitization degree associated with the perfect nanotube structure while the D-band arises from structural defects described above, including amorphous (non-graphitic) carbons incorporated into the nanotube structure. Therefore, the plot of G-band to D-band peak ratios versus the nanotube length shown in Figure 3b indicates that those nanotube segments at the top tube end formed at the initial stage of the "bottom growth" process have a relatively low structural defect content because the catalyst activity is usually high to start with.[3] The observed decrease in the G-band to D-band peak ratio along the nanotube length from the top to bottom tube end (Figure 3) is presumably due to a decrease in the activity of catalyst nanoparticles with increasing growth time. Generally speaking, the rate balance between the amorphous carbon deposition on the catalyst surface and its removal by water vapor/H_2 is a key factor to keep the catalyst active for the long time growth of the super-long nanotubes. Comparing with the amorphous carbon removal, however, the rate of amorphous carbon deposition normally increases with the nanotube growth time. This eventually leads to a continuous decrease in the catalyst activity until the termination of nanotube growth. As a consequence, more structural defects are introduced at a later stage of the nanotube growth; consistent with our experimental observation shown in Figure 3.

To understand the possible effects of the structural defect distribution on the electrochemical property along the nanotube length, we performed length-specific cyclic voltammetric measurements along the 5-mm-long SLVA-DWNTs using an $Fe(CN)_6^{4-/3-}$ couple as an electrochemical probe. Typically, the redox reaction of the $Fe(CN)_6^{4-/3-}$ couple proceeds with one-electron transfer in a quasi-reversible way, providing a convenient probe to monitor the structural defects of carbon-based electrode surfaces by following their effects on the electro-

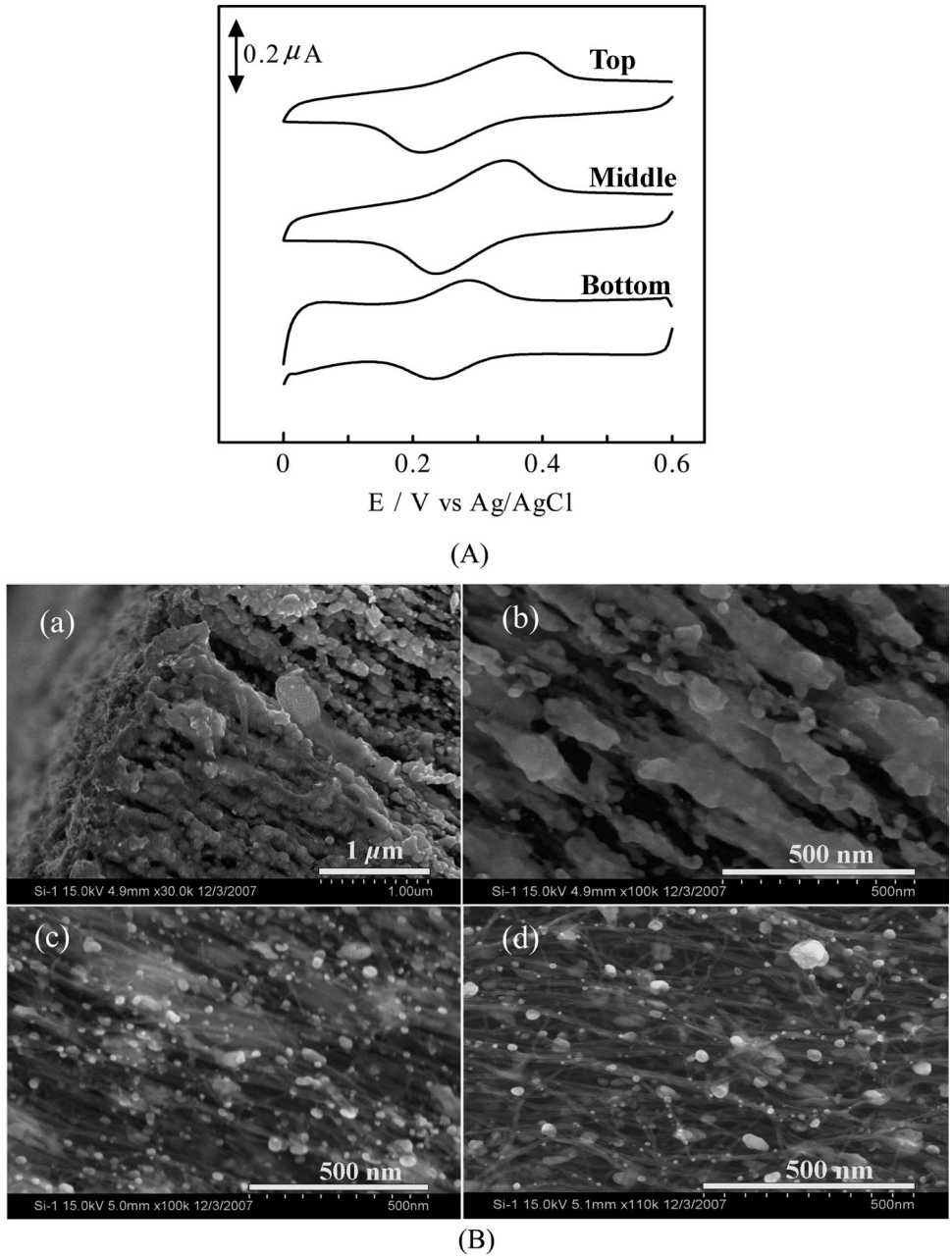

Figure 4. (A) Typical cyclic voltammograms obtained at the top, middle, and bottom end of the SLVA-DWNT bunch in 0.1 M KCl containing 1 mM $K_3Fe(CN)_6$. Scan rate: 0.1 V s^{-1} unless otherwise stated. (B) Scanning electron microscope images of the Au-coated long SLVA-DWNTs at different length portions: (a) the top end, (b) 1 mm below the top end, (c) 3 mm below the top end, and (d) at the bottom end.

chemical reaction rate. In the present study, electrochemical measurements were performed using a computer-controlled potentiostat (CHI 760C, CH Instrument) in a typical three-electrode cell. The SLVA-DWNT electrodes were prepared by connecting one end of the super-long nanotube bunch to a copper wire with silver epoxy conducting adhesive, followed by air drying. The SLVA-DWNT electrode thus prepared was then used as a working electrode, an Ag/AgCl (3 M KCl-filled) electrode was used as the reference electrode, and a platinum wire was used as the counter electrode. A 0.1 M KCl solution was used as the supporting electrolyte. To measure the voltammetric responses for each of the two nanotube ends (i.e., top or bottom), a micromanipulator was used to vertically hold the copper wire that connected to the SLVA-DWNT bunch, and to move down the free-end of the DWNT electrode carefully toward the electrolyte solution until a well-defined voltammetric cycle was recorded. For electrochemical measurements on the middle part of the super-long DWNT bunch, the two nanotube ends were insulated by coating with a polystyrene solution in toluene (40 wt %) and dried in air. The effectiveness of the polystyrene masking was checked by fully coating the nanotube with polystyrene under the same conditions, which showed no electrochemical signal at all.

Figure 4A shows typical cyclic voltammograms of 1.0 mM $K_3Fe(CN)_6$ at the top, middle, and bottom part of a 5-mm-long SLVA-DWNT bunch (cf. Figure 3) with a scan rate of 0.1 V s^{-1}. The peak-to-peak separation (i.e., ΔE_p) in the cyclic voltammogram recoded for the bottom part of the SLVA-DWNTs kept constant (ca. 59 mV) at the scan rates ranging from 10 to 300 mV s^{-1}, indicating a Nernst process with a very fast electron transfer. In contrast, the corresponding cyclic voltammograms for the middle and the top parts of the SLVA-DWNTs showed much larger peak-to-peak separations (i.e., $\Delta E_p = 106$ and 160 mV, respectively), suggesting a decrease

in the electron transfer rate along the nanotube length from the bottom to top of the super-long nanotubes. In view of the fact that the CNT-based electrochemistry is often dominated by the presence of structural defects (e.g., delocalized carbons, oxidized sites),[15–18] the electrcochemcial measurements indicate, once again, that the content of structural defects decreases along the nanotube length from the bottom to top end for the SLVA-DWNTs.

The above results prompted us to deposit metal nanoparticles along the nanotube length with a gradient packing density by, for example, substrate-enhanced electroless deposition (SEED) of Au nanoparticles.[19] As discussed in our earlier publications,[19,20] the SEED method allows metal nanoparticles to be deposited in the defect-free regions on nanotube surfaces. By simply immersing a long SLVA-DWNT bunch supported by a Cu foil into an aqueous solution of $HAuCl_4$ (2 mM), Au nanoparticles were spontaneously deposited in the defect-free areas along the nanotube length. The defect distribution on the nanotube surface along the nanotube length could thus be correlated with the distribution of Au nanoparticles, which can be visualized on an electron microscope. Figure 4B shows SEM images for the 5-mm-long SLVA-DWNTs decorated with Au particles deposited by the SEED method.[19,20] As can be seen, a nanotube-length-specific deposition of Au particles was indeed observed with the Au particles densely packed along the top part of the SLVA-DWNTs (Figure 4B(a)). The packing density of the Au particles decreased along the nanotube length from the top to bottom end (Figure 4B(a−d)). In the SEED process, it is known that electrons from the Cu substrate transfer through the nanotube surface to reduce Au^{3+} ions into the Au particles.[19,20] In this particular case, therefore, Au particles are preferentially deposited in defect-free areas on the nanotube surface. Hence, the structural defect gradient measured above by Raman spectroscopy and electrochemical cyclic voltammetry is responsible for the observed decrease in packing density of the SEED-deposited Au particles along the nanotube length from the top to bottom end. A trivial explanation of the observed packing density gradient of the Au particles along the nanotube length related to possible nanotube packing density changes along their length and/or variable diffusion rates of Au^{3+} ions toward different parts of the nanotubes can be ruled out based on the fact that almost all of the constituent nanotubes have a uniform length in the SLVA-DWNT array (Figure 1a), and that the nanotube bunch was lying flat on the Cu substrate during the SEED process.[19,20]

In summary, we have demonstrated for the first time that there is a concentration gradient of structural defects along the nanotube length for super-long, vertically aligned CNTs prepared by water-assisted CVD growth. Owing to the decay of the catalyst reactivity with the growth time, the SLVA-DWNT arrays produced by the "bottom growth" process showed an increase in structural defect content along the nanotube length from the top to bottom end. The newly detected defect content gradient allowed us to tune the nanotube electrochemistry along its length and to deposit metal particles in a length-specific fashion. The super-long carbon nanotubes functionalized with metal nanoparticles with a packing density gradient along the nanotube length could have potential applications in various optoelectronic devices requiring tunable electronic and surface plasmon resonance properties.

Acknowledgment. We thank the AFOSR (FA9550-06-1-0384), NSF (CMS-0609077, 0708055), AFRL/ML, Wright Brothers Institute, and Dayton Development Collations for financial support. We acknowledge the NEST Lab at UD for the access of SEM and TEM facilities.

References and Notes

(1) Chakrabarti, S.; Kume, H.; Pan, L.; Nagasaka, T.; Nakayama, Y *J. Phys. Chem. C* **2007**, *111*, 1929.
(2) Chakrabarti, S.; Nagasaka, T.; Yoshikawa, Y.; Pan, L.; Nakayama, Y. *J. J. Appl. Phys. Express Lett.* **2007**, *45*, L720.
(3) Hata, K.; Futaba, D. N.; Mizuno, K.; Namai, T.; Yumura, M.; Iijima, S. *Science* **2004**, *306*, 1362.
(4) Veedu, V. P.; Cao, A.; Li, X.; Ma, K.; Soldano, C.; Kar, S.; Ajayan, P. M.; Ghasemi-Nejhad, M. N. *Nat. Mater.* **2006**, *5*, 457.
(5) Ajayan, P. M.; Tour, J. M. *Nature* **2007**, *447*, 1066.
(6) Qu, L.; Peng, Q.; Dai, L.; Spinks, G.; Wallace, G.; Baughman, R. H. *MRS Bull.* **2008**, *33*, 215.
(7) Wei, C.; Dai, L.; Roy, A.; Benson-Tolle, T. *J. Am. Chem. Soc.* **2005**, *127*, 10806.
(8) Snow, E. S.; Perkins, F. K.; Houser, E. J.; Badescu, S. C.; Reinecke, T. L. *Science* **2005**, *307*, 1942.
(9) Bachtold, A.; Hadley, P.; Nakanishi, T.; Dekker, C. *Science* **2001**, *294*, 1317.
(10) Chen, Z.; Appenzeller, J.; Lin, Y.; Sippel-Oakley, J.; Rinzler, A. G.; Tang, J.; Wind, S. J.; Solomon, P. M.; Avouris, P. *Science* **2006**, *311*, 1735.
(11) Odom, T. W.; Huang, J. L.; Kim, P.; Lieber, C. M. *J. Phys. Chem. B* **2001**, *104*, 2794.
(12) Louies, S. G. *Top. Appl. Phys.* **2001**, *80*, 113.
(13) Bahr, J. L.; Yang, J.; Kosynkin, D. V.; Smalley, R. E. *J. Am. Chem. Soc.* **2001**, *123*, 6536.
(14) Liu, J.; Rinzler, A. G.; Dai, H. J.; Smalley, R. E. *Science* **1998**, *280*, 1253.
(15) Gooding, J. J. *Electrochim. Acta* **2005**, *50*, 3049.
(16) Wildgoose, G. G.; Banks, C. E.; Compton, R. G. *Small* **2006**, *2*, 182–193.
(17) Banks, C. E.; Davies, T. J.; Wildgoose, G. G.; Compton, R. G. *Chem. Commun.* **2005**, *7*, 829.
(18) Gong, K.; Yan, Y.; Zhang, M.; Su, L.; Xiong, S.; Mao, L. *Anal. Sci.* **2005**, *21*, 1383.
(19) Qu, L.; Dai, L. *J. Am. Chem. Soc.* **2005**, *127*, 10806.
(20) Qu, L.; Dai, L.; Osawa, E. *J. Am. Chem. Soc.* **2006**, *128*, 5523.

JP802059T